

# Coexistence of 3D and quasi-2D Fermi surfaces driven by orbital selective Kondo scattering in $\text{UTe}_2$

Byungkyun Kang,<sup>1,\*</sup> Myoung-Hwan Kim,<sup>2</sup> and Chul Hong Park<sup>3</sup>

<sup>1</sup>*College of Arts and Sciences, University of Delaware, Newark, DE 19716, USA*

<sup>2</sup>*Department of Physics and Astronomy, Texas Tech University, Lubbock, Texas 79409, USA*

<sup>3</sup>*Research Center of Dielectric and Advanced Matter Physics, Pusan National University, Busan 46240, Republic of Korea*

The 3D Fermi surface, along with a chiral in-gap state and a Majorana zero energy state, is suggested to play a crucial role in the topologically nontrivial superconductivity in  $\text{UTe}_2$ . However, conflicting experimental observations of the 2D Fermi surface raise questions about topological superconductivity. By combining ab initio many-body perturbation GW theory and dynamical mean-field theory based on Feynman diagrams, we discovered the coexistence of two orbital dependent Fermi surfaces, both centered at the  $\Gamma$  point in the Brillouin zone, which are heavily influenced by the orbital-selective Kondo effect. At high temperature, both Fermi surfaces exhibit 3D nature with weak spectral weight due to incoherent Kondo hybridization. Upon cooling down to 25 K, due to the pronounced Kondo coherence, while one Fermi surface remains a robust 3D Fermi surface, the other transforms surprisingly into a quasi-2D Fermi surface, which should be responsible for the experimental observation of 2D character. Our results suggest that the 3D Fermi surface should exist at low temperature for the topological superconductivity. Our findings call for further investigation of the interplay between the two orbital-dependent  $\Gamma$ -centered Fermi surfaces.

## INTRODUCTION

The plausibility of topological superconductivity in  $\text{UTe}_2$  has been a topic of considerable contention, contingent upon the presence of a three-dimensional (3D) Fermi surface. Recent scanning tunneling microscopy/spectroscopy measurements have revealed the presence of a chiral in-gap state and Majorana zero energy states in  $\text{UTe}_2$  [1], providing evidence for the existence of a 3D Fermi surface. Two studies using angle-resolved photoemission spectroscopy, while presenting contrasting results, have suggested the existence of a possible 3D Fermi surface measured at 20 K [2, 3]. This is further supported by quantum oscillation measurements below 1.2 K, which show coexistence of 3D and 2D Fermi surface pockets [4]. However, recently, conflicting results have been reported. Fermi surface measurements using the de Haas-van Alphen effect below 200 mK [5] and high magnetic field magneto-conductance oscillations below 4.2 K [6] identified only quasi-two-dimensional (quasi-2D) Fermi surface. One of main ingredient for the topological superconductivity is 3D Fermi surface since quasi-2D cylindrical Fermi surface can't support topologically nontrivial state. These complicated phenomena are not yet explained by theoretical studies. Tight binding model [7], density functional theory (DFT) [2], and DFT combined with dynamical mean field theory (DMFT) [8] all predicted a 3D Fermi surface centered at the  $\Gamma$  point in the Brillouin zone. On the other hand, DFT+ $U$  calculations [3, 9, 10] have reported only non- $\Gamma$ -centered quasi-2D cylindrical sheet of the Fermi surface. There is a pressing demand for a microscopic careful examination of Fermi surface topology from a first-principles many-body perspective to understand topological superconductivity in  $\text{UTe}_2$ . In this work, it is shown that orbital dependent Kondo hybridization plays an important role in the complex reconstruction of both

$\Gamma$ -centered 3D and quasi-2D Fermi surfaces, on top of a non- $\Gamma$ -centered quasi-2D cylindrical sheet of the Fermi surface.

The enigmatic properties of  $\text{UTe}_2$  extend beyond its unconventional superconductivity, as evidenced by its re-entrant behavior that is contingent upon the orientation of the applied magnetic field [11–13]. This intriguing phenomenon can be elucidated by the anisotropic electronic structure, as demonstrated by the orbital selective Kondo effect [14, 15]. Furthermore, under high pressure,  $\text{UTe}_2$  has been observed to exhibit long-range magnetic ordering [16–19]. This has been attributed to the momentum-dependent  $f$ - $d$  Kondo hybridization. The coherent Kondo hybridization under high pressure leads to the delocalization of Bloch-like  $U$ - $5f$  quasiparticles and the van Hove singularity, which is the origin of the magnetic moment [20]. These studies demonstrate that the Kondo effect has a significant impact on the electronic structure of  $\text{UTe}_2$ .

In the Kondo lattice  $\text{UTe}_2$ , the intense local magnetic moment of the  $U$ - $5f$  orbitals is influenced by the Kondo hybridization with conduction electrons at the Fermi level. Consequently, the shape and properties of the Fermi surface are significantly influenced by the Kondo scale and the specific orbitals involved. To describe the Kondo effect, a phenomenon arising from strong electron correlation, an ab-initio many-body method is necessary for accurately depicting the Fermi surface. The ab-initio many-body approach has yielded a calculated static  $U(\omega = 0)$  value of 3.29 eV for  $\text{UTe}_2$  [14, 20], indicating a moderate strength of Mottness. Moreover, it has been shown that  $\text{UTe}_2$  does not display a pseudogap up to 6000 K [14], suggesting its similarity to a Hund's metal, where the exchange interaction  $J$  dominates over  $U$  [21, 22]. Thus, the presence of metallic  $U$ - $5f$  spectral weight in the vicinity of the Fermi level remains prominent at elevated temperatures, resulting in incoherent Kondo scattering. In general, Kondo scattering becomes more coherent as the temperature decreases. However, the evolution of the Fermi surface resulting from orbital selective Kondo scattering is unknown.

A common characteristic shared by unconventional super-

\* bkang@udel.edu

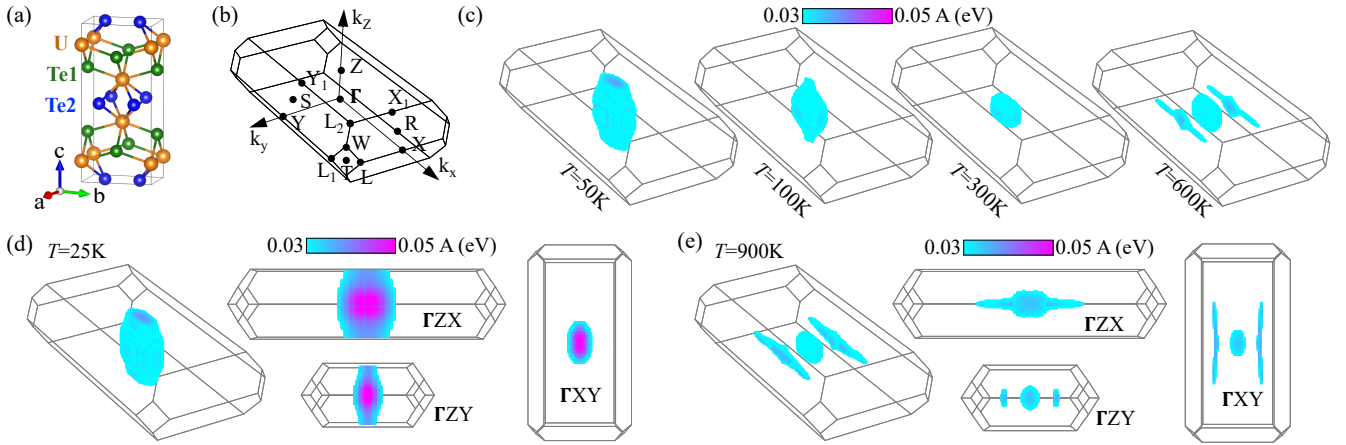


FIG. 1. (a) Crystal structure of  $UTe_2$ . (b) The first Brillouin zone. (c)  $Te2-5p$  state of  $|j = 3/2, j_z = -3/2\rangle$  projected Fermi surface in the Brillouin Zone.  $Te2-5p$  state of  $|j = 3/2, j_z = -3/2\rangle$  projected Fermi surface and its cross section at  $T=25$  K (a) and  $T=900$  K (b). In (c), (d), and (e), the same spectral weight, as noted by the color bar in (d), was used.

conductors based on copper and iron is the quasi-2D Fermi surface, which strongly restricts the possible pairing symmetries [23, 24]. In the case of  $UTe_2$ , the quasi-2D Fermi surface is likely to play a significant role in the unconventional superconductivity. Although the quasi-2D Fermi surface does not contribute to the nontrivial topological invariant, the emergence of a 3D Fermi surface could potentially host topological superconductivity through odd-parity pairings [8].

## RESULTS

In this work, we reveal, through ab-initio many-body calculations that explicitly include the Kondo effect, the coexistence of 3D and quasi-2D Fermi surfaces centered at the  $\Gamma$  point at low temperatures, due to the orbital selective Kondo effect. In the direction of the  $c$  axis, incoherent Kondo hybridization primarily involving  $Te-5p$  and  $U-5f$  orbitals gives rise to a 3D Fermi surface centered at the  $\Gamma$  point at high temperatures. Interestingly, as the temperature decreases, the quasi-2D Fermi surface is found to emerge due to the enhancement of the coherent Kondo hybridization. Additionally, there is an incoherent dispersive 3D Fermi surface comprising  $U-6d$  states at high temperature. Upon cooling, this 3D Fermi surface becomes more coherent with pronounced spectral weight. Our results support the quantum oscillation measurements that demonstrate the coexistence of 2D and 3D Fermi surfaces [4]. We examined the electronic structure of  $UTe_2$  by using ab-initio linearized quasiparticle self-consistent GW + dynamical mean field theory (LQSGW+DMFT) method [25]. This method enables us to accurately determine the temperature-dependent electronic structure of strongly correlated materials without any subjective judgment. Aside from adopting an experimental lattice parameter, we explicitly compute all other quantities, such as double-counting energy and Coulomb interaction tensor. The LQSGW+DMFT method has been used to investigate

the Kondo effect in compounds based on actinides and lanthanides [14, 20, 26, 27].

### Transition from 3D to quasi-2D Fermi surface of $Te2-5p$

The crystal structure of the orthorhombic phase (Immm)  $UTe_2$  [28] is described in Fig. 1a. The high symmetry k-points in the first Brillouin zone are shown in Fig. 1b.  $UTe_2$  consists of two Te atoms with Wyckoff positions 4j (Te1) and 4h (Te2).  $Te2-5p$ -orbitals were shown to be responsible for the Kondo effect along the  $c$  axis [14]. Here, we show that the Fermi surface projected by the  $Te2-5p$  state of the  $|j = 3/2, j_z = -3/2\rangle$  in the Brillouin zone significantly changes with a decrease of temperature, as shown in Fig. 1c. It is remarkable that as the temperature is lowered, the Fermi surface transforms from the closed 3D one to the open 2D one. At high  $T$  of 600 K, a 3D oblate Fermi surface forms at  $\Gamma$ , whereas at low  $T$  of 50 K, it transforms to be quasi-2D cylindrical. In Fig. 1d and e, more details are compared by the cross sections of the Fermi surface between  $T = 900$  K and 25 K. Both Fermi surfaces exhibit densely packed spectral weight, unlike 3D pocket Fermi surface observed in quantum oscillations measurements [4]. At 900 K, the spectral weight on the Fermi surface is broadened and incoherent, whereas at 25 K, the spectral weight is more increased along the  $\Gamma$ -Z high symmetry direction. As an orbital selective Kondo lattice, the  $Te2-5p$  states of  $|j = 3/2, j_z = \pm 3/2\rangle$  hybridize with the  $U-5f$  states of  $|j = 5/2, j_z = \pm 5/2\rangle$ , which are responsible for the Kondo effect along the  $c$  axis [14]. On the Fermi surface project by  $U-5f$  states of  $|j = 5/2, j_z = \pm 5/2\rangle$ , the spectral weight is dispersive across the entire Brillouin zone. This indicates that the flat  $U-5f$  electrons lead to the Kondo scattering of  $Te2-5p$ , and the 3D shape of the Fermi surface is mostly contributed by  $Te2-5p$ .

The  $Te2-5p$ -driven spectral weight on the Fermi surface increases at low temperature of 25 K, and the DOS of the  $U-5f$

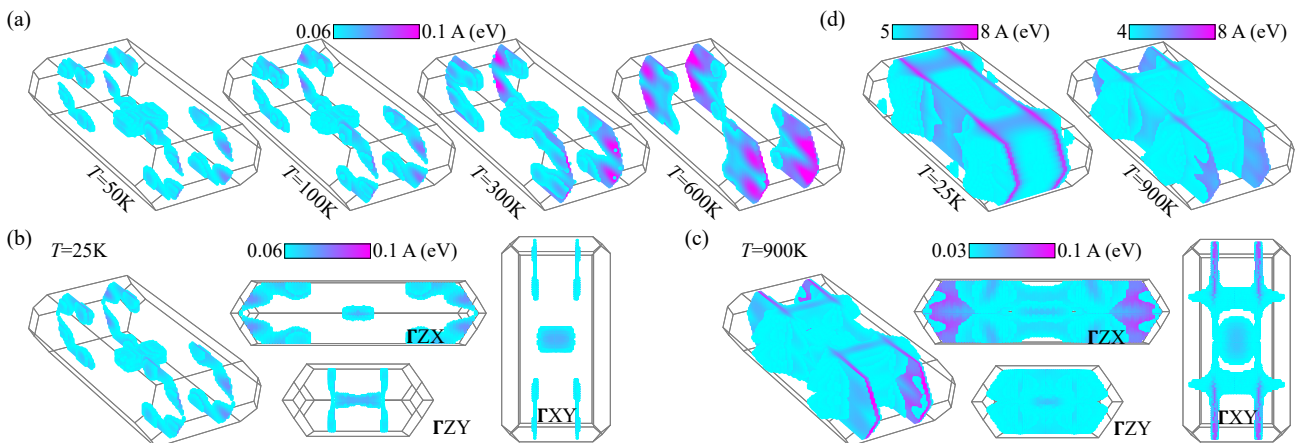


FIG. 2. (a) U-6d states of  $|j = 3/2, j_z = -3/2\rangle$  projected Fermi surface in the Brillouin Zone. U-6d states of  $|j = 3/2, j_z = -3/2\rangle$  projected Fermi surface and its cross section at  $T=25$  K (b) and  $T=900$  K (c). (d) The Fermi surface of  $UTe_2$  at  $T=25$  K and 900 K.

states of  $|j = 5/2, j_z = \pm 5/2\rangle$  at the Fermi level exhibit a progression in the formation of a quasiparticle peak at low  $T$  below 50K [14]. These findings suggest that the coherent Kondo resonance between the Te2-5p states of  $|j = 3/2, j_z = \pm 3/2\rangle$  and the U-5f states of  $|j = 5/2, j_z = \pm 5/2\rangle$  drives the transformation of the 3D Fermi surface into the quasi-2D Fermi surface.

#### Enhanced 3D Fermi surface of U-6d

We found that the U-6d states of  $|j = 3/2, j_z = \pm 3/2\rangle$  give rise to a 3D Fermi surface centered at  $\Gamma$ . Figure 2a shows that the 3D Fermi surface of the U-6d states of  $|j = 3/2, j_z = -3/2\rangle$  centered at  $\Gamma$ . At 900 K, the 3D Fermi surface is invisible within the given range of spectral weight. Upon cooling, the 3D Fermi surface appears due to stronger spectral weight, with a slightly varying size. Figure 2b shows the cross sections of the Fermi surface at 25 K. It exhibits a dumbbell shape, unlike the oval shape obtained from LDA+DMFT [8]. As shown in Fig. 2c, the 3D Fermi surface appears at a high temperature of 900 K. The spectral weight is weak and dispersive, making it visible only at a lower range of spectral weight ( $< 0.06$  A (eV)).

To determine the Fermi surface topology, we calculated the Fermi surface for all orbitals, as shown in Fig. 2d. The calculated Fermi surface is non- $\Gamma$ -centered quasi-2D cylindrical sheet at  $T=900$  K and consists mainly of U-6d (see Fig. 2c) and dispersive U-5f orbitals. The non- $\Gamma$ -centered quasi-2D cylindrical sheet of Fermi surface is similar to that obtained by the DFT+ $U$  method [3, 10], because the majority of the cylindrical Fermi surface is composed of weakly correlated U-6d and Te-5p bands. At  $T=25$  K, the Fermi surface still retains its quasi-2D feature. However, the Fermi surface along the  $k_x$  axis becomes more coherent, while the Fermi surface along the  $k_y$  axis becomes more dispersed compared to the Fermi surface at  $T=900$  K. The dispersion is attributed to the kink-like band structure along the  $\Gamma$ -X high symmetry line

at  $T=25$  K, which is caused by a stronger Kondo hybridization between U-6d and a subgroup of U-5f [14] compared to  $T=900$  K, as shown in Fig. 3a. The  $\Gamma$  centered Te2-5p projected quasi-2D Fermi surface and U-6d projected 3D Fermi surface are not visible in Fig. 2d due to their relatively small spectral weight. Nonetheless, the coexistence of the 3D and quasi-2D Fermi surfaces centered at  $\Gamma$  is apparent in our orbital projected Fermi surface.

#### Coexistence of 3D and quasi-2D Fermi surface driven by orbital selective Kondo scattering

The calculated spectral functions and orbital-projected density of states (DOS) of  $UTe_2$  at  $T=25$  K and 900 K are compared in Fig 3a. At 900 K, the U-5f-driven bands around -0.2 eV exhibit an incoherent feature, which shifts towards the Fermi level at 25 K, forming a strong Kondo peak with a kink band structure. This is reminiscent of the formation of a quasiparticle peak upon cooling, which leads to the formation of a Kondo cloud [27, 29]. A distinctive feature of  $UTe_2$  is that the U-5f-orbitals form a metallic band at high temperatures, reaching up to 6000 K [14].  $UTe_2$  is known as a high temperature Kondo lattice with a Kondo scale of approximately 500 K, as estimated from the behavior of the U-5f DOS and local angular momentum susceptibility [14].

As shown in Fig 3a, the U-5f peak is slightly below the Fermi level at 900 K, and the dispersive U-5f metallic bands are extended to the Fermi level. This gives rise incoherent Kondo hybridization between U-5f and conduction electrons of Te2-5p and U-6d. As shown in Fig. 3b, the incoherent Kondo hybridization between the Te2-5p state of  $|j = 3/2, j_z = -3/2\rangle$  and the dispersive U-5f bands results in the appearance of dispersive Te2-5p state  $|j = 3/2, j_z = -3/2\rangle$  bands along the  $\Gamma$ -Z direction at a temperature of 2000 K. The dispersive band of Te2-5p state  $|j = 3/2, j_z = -3/2\rangle$  also appears along the  $\Gamma$ -X and  $\Gamma$ -Y high symmetry lines. These results indicate that incoherent Kondo scattering occurs

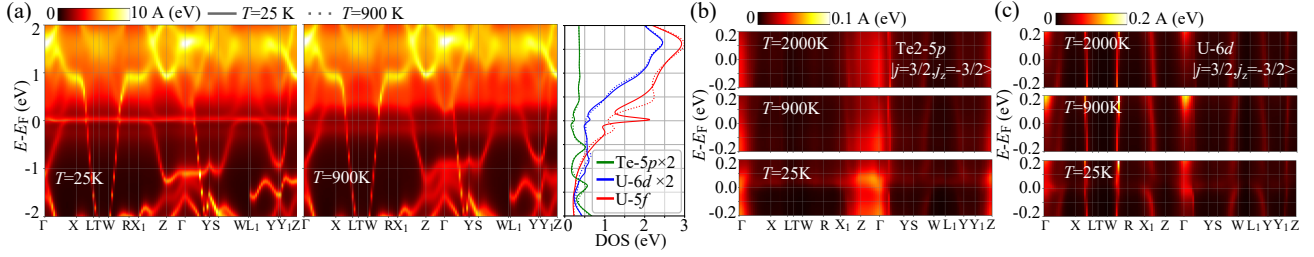


FIG. 3. (a) The calculated spectral functions and density of states for  $\text{UTe}_2$  at  $T=25$  K (solid lines) and 900 K (open). Te-5p state of  $|j = 3/2, j_z = -3/2\rangle$  (b) and U-6d states of  $|j = 3/2, j_z = -3/2\rangle$  (c) projected spectral functions at  $T=2000, 900,$  and 25 K.

in all directions from  $\Gamma$ , resulting in the formation of the 3D Fermi surface centered at  $\Gamma$  at high temperatures. Upon cooling, the coherent features of Kondo scattering become more pronounced, resulting in a brighter spectral weight. In particular, the coherent character at 25 K is strongly enhanced along the  $\Gamma$ -Z direction, which leads to the quasi-2D Fermi surface. This is observed as a cylindrical Fermi surface, as shown in Fig. 1d.

As shown in Fig. 3c, the incoherent Kondo hybridization between the U-6d state of  $|j = 3/2, j_z = -3/2\rangle$  and the dispersive U-5f bands results in the appearance of dispersive U-6d state of  $|j = 3/2, j_z = -3/2\rangle$  bands along the  $\Gamma$ -X, Y, and Z directions at a temperature of 2000 K. Upon cooling, the coherent features of Kondo scattering become more pronounced, resulting in a brighter spectral weight in the vicinity of the Fermi level. In particular, the coherent character at 25 K is strongly enhanced along the  $\Gamma$ -Y direction, leading to the dumbbell shaped 3D Fermi surface, as shown in Fig. 2b.

## DISCUSSION

We discovered that Kondo hybridization leads to Fermi surface reconstruction in  $\text{UTe}_2$ . Interestingly, it is found that as the temperature decreases down to 25 K, the enhanced orbital selective Kondo coherence leads to the coexistence of a  $\Gamma$ -centered strong 3D Fermi surface and a quasi-2D Fermi surface, which gives a clear explanation for the observations of coexistence of 3D or 2D feature [4].

The two  $\Gamma$ -centered Fermi surfaces are comprised of conducting electrons from U-6d and Te-5p. They are subject to orbital-selective Kondo scattering with U-5f. Our previous study in the same manner as this work, which predicted the Kondo scale using the calculated density of states and susceptibility, explains the anisotropic electronic resistivity measurements [14, 15]. This should be the evidence for the Fermi surface reconstruction originating from the Kondo effect. However, in the Kondo effect, since the localized U-5f electrons dominate the Fermi surface, forming a peak in density of states at Fermi level at low temperatures, the spectral weight of both  $\Gamma$ -centered Fermi surfaces should be relatively weak, and their contribution to the Hall effect for the Fermi surface reconstruction should be limited [30]. Quantitative research on the effect of the two Fermi surfaces on the Hall effect de-

mands further study.

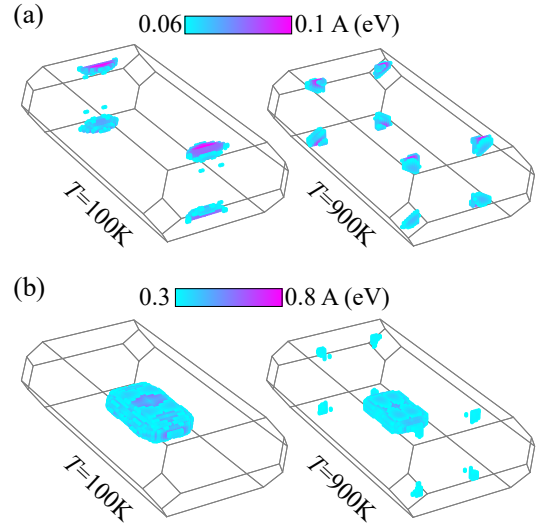


FIG. 4. The calculated orbital projected Fermi surface in the Brillouin Zone without spin-orbit coupling at  $T=100$  and 900 K. (a) Te-5p state of  $|l = 1, m = 0\rangle$  projected Fermi surface. (b) U-6d states of  $|l = 2, m = 2\rangle$  projected Fermi surface.

Two DFT+DMFT studies on  $\text{UTe}_2$  have been conducted, both of which do not take spin-orbit coupling (SOC) into account [31, 32]. These studies reveal a flat U-5f peak that is hybridized with conduction electrons at 10 K, while noting that the peak diminishes at 200 K. This indicates that the Kondo scale in the non-SOC system is lower than 500 K in the SOC system [14]. By employing LQSGW+DMFT, our study revealed that in the absence of SOC, the uranium atom undergoes strong oxidation, with the U-5f occupancy being 1.17, considerably lower than the 2.27 observed in the SOC simulation [14]. This pronounced local magnetic moment is critical for Kondo scattering, implying that Kondo scaling is significantly reduced in the non-SOC system. Figure 4 show the Fermi surface of  $\text{UTe}_2$  without considering SOC within LQSGW+DMFT. In the non-SOC system, the U-6d projected Fermi surface exhibits a 3D character. In contrast, the Te-5p projected Fermi surface shows no evidence of a  $\Gamma$ -centered Fermi surface. This suggests that SOC plays a crucial role

in the reconstruction of the quasi 2D Fermi surface of  $\text{Te}_2\text{-}5p$  at low temperatures, as shown in Fig. 1, where the SOC is explicitly included. The significant local  $U\text{-}5f$  magnetic moment, originating from the strong SOC, leads to a flat  $U\text{-}5f$  band at the Fermi level. At sufficiently low temperatures, the flat  $U\text{-}5f$  band undergoes Kondo hybridization with  $\text{Te}_2\text{-}5p$  along the  $c$ -axis, leading to the quasi-2D Fermi surface.

Although the spectral weight of both  $\Gamma$ -centered Fermi surfaces are weaker than that of the non- $\Gamma$ -centered cylindrical Fermi surface, they should be observable for a short period of time. As the temperature decreases below 25 K, the Kondo coherence should become stronger. Consequently, it is expected that both the  $\Gamma$ -centered 3D and quasi-2D Fermi surfaces should be more observable and have longer lifetimes below 25 K, which our methods can't access due to the sign problem in Monte Carlo simulations.

Our results show that the coexistence behavior of 3D and quasi-2D Fermi surfaces can be clearly understood by the evolution of orbital selective Kondo hybridization at low temperature. It gives an explanation to inconsistent experimental observations due to orbital and temperature dependent Fermi surfaces. The  $\Gamma$ -centered 3D Fermi surface should potentially host topological superconductivity, as has been suggested. The impact of the quasi-2D Fermi surface centered around  $\Gamma$  on topological superconductivity should be investigated in future studies.

## METHODS

### A. LQSGW and DMFT calculations

The electronic structure of  $\text{UTe}_2$  was calculated using the *ab-initio* linearized quasiparticle self-consistent GW (LQSGW) combined with dynamical mean field theory (DMFT) [25, 33]. Classified under the Immm (No. 71) space group, this material's structure has been confirmed by

previous investigations [28, 34]. The LQSGW+DMFT approach is a streamlined variant of the GW+EDMFT method [35–39], wherein LQSGW techniques [40, 41] are employed to derive the electronic structure. DMFT is then used to correct any discrepancies in the local GW self-energy [42–44]. In this study, we utilized experimentally measured lattice constants ( $a = 4.1611$ ,  $b = 6.1222$ ,  $c = 13.955$  Å) [28] and computed all other necessary parameters, including double-counting energy and the Coulomb interaction tensor. Local self-energies for  $U\text{-}5f$  and  $U\text{-}6d$  were derived by solving two distinct single impurity models using the continuous time quantum Monte Carlo (CTQMC) method. The LQSGW+DMFT framework was implemented with the ComDMFT code [25], while the LQSGW calculations were performed using the FlapwMBPT code [41]. Further details can be found in the Supplementary Methods section.

## ACKNOWLEDGMENTS

We acknowledge the High Performance Computing Center (HPCC) at Texas Tech University for providing computational resources that have contributed to the research results reported within this paper. C.H. Park acknowledges the support by the National Research Foundation of Korea (NRF) grant (Grant No. NRF-2022R1A2C1005548).

**Competing Interests** The authors declare no competing interests.

**Data availability** The data that support the findings of this study are available from the corresponding authors upon reasonable request.

**Author contributions** B.K. designed the project. B.K. performed the calculations and conducted the data analysis. All authors wrote the manuscript, discussed the results, and commented on the paper.

- 
- [1] L. Jiao, S. Howard, S. Ran, Z. Wang, J. O. Rodriguez, M. Sigrist, Z. Wang, N. P. Butch, and V. Madhavan, Chiral superconductivity in heavy-fermion metal  $\text{UTe}_2$ , *Nature* **579**, 523 (2020).
  - [2] S.-i. Fujimori, I. Kawasaki, Y. Takeda, H. Yamagami, A. Nakamura, Y. Homma, and D. Aoki, Electronic structure of  $\text{UTe}_2$  studied by photoelectron spectroscopy, *J. Phys. Soc. Jpn.* **88**, 103701 (2019).
  - [3] L. Miao, S. Liu, Y. Xu, E. C. Kotta, C.-J. Kang, S. Ran, J. Paglione, G. Kotliar, N. P. Butch, J. D. Denlinger, and L. A. Wray, Low energy band structure and symmetries of  $\text{UTe}_2$  from angle-resolved photoemission spectroscopy, *Phys. Rev. Lett.* **124**, 076401 (2020).
  - [4] C. Broyles, Z. Rehfuss, H. Siddiquee, J. A. Zhu, K. Zheng, M. Nikolo, D. Graf, J. Singleton, and S. Ran, Revealing a 3D Fermi Surface Pocket and Electron-Hole Tunneling in  $\text{UTe}_2$  with Quantum Oscillations, *Phys. Rev. Lett.* **131**, 036501 (2023).
  - [5] A. Eaton, T. Weinberger, N. Popiel, Z. Wu, A. Hickey, A. Cabala, J. Pospíšil, J. Prokleška, T. Haidamak, G. Bastien, *et al.*, Quasi-2D Fermi surface in the anomalous superconductor  $\text{UTe}_2$ , *Nat. Commun.* **15**, 223 (2024).
  - [6] T. I. Weinberger, Z. Wu, D. E. Graf, Y. Skourski, A. Cabala, J. Pospíšil, J. Prokleška, T. Haidamak, G. Bastien, V. Sechovský, G. G. Lonzarich, M. Vališka, F. M. Grosche, and A. G. Eaton, Quantum Interference between Quasi-2D Fermi Surface Sheets in  $\text{UTe}_2$ , *Phys. Rev. Lett.* **132**, 266503 (2024).
  - [7] J. Ishizuka and Y. Yanase, Periodic Anderson model for magnetism and superconductivity in  $\text{UTe}_2$ , *Phys. Rev. B* **103**, 094504 (2021).
  - [8] H. C. Choi, S. H. Lee, and B.-J. Yang, Correlated normal state fermiology and topological superconductivity in  $\text{UTe}_2$ , *Commun. Phys.* **7**, 273 (2024).
  - [9] J. Ishizuka, S. Sumita, A. Daido, and Y. Yanase, Insulator-metal transition and topological superconductivity in  $\text{ute}_2$  from a first-principles calculation, *Phys. Rev. Lett.* **123**, 217001 (2020).

- (2019).
- [10] Y. Xu, Y. Sheng, and Y.-f. Yang, Quasi-two-dimensional fermi surfaces and unitary spin-triplet pairing in the heavy fermion superconductor  $UTe_2$ , *Phys. Rev. Lett.* **123**, 217002 (2019).
- [11] S. Ran, I.-L. Liu, Y. S. Eo, D. J. Campbell, P. M. Neves, W. T. Fuhrman, S. R. Saha, C. Eckberg, H. Kim, D. Graf, *et al.*, Extreme magnetic field-boosted superconductivity, *Nat. Phys.* **15**, 1250 (2019).
- [12] S. Ran, H. Kim, I.-L. Liu, S. R. Saha, I. Hayes, T. Metz, Y. S. Eo, J. Paglione, and N. P. Butch, Enhancement and reentrance of spin triplet superconductivity in  $UTe_2$  under pressure, *Phys. Rev. B* **101**, 140503 (2020).
- [13] D. Aoki, K. Ishida, and J. Flouquet, Review of U-based ferromagnetic superconductors: Comparison between  $UGe_2$ ,  $URhGe$ , and  $UCoGe$ , *J. Phys. Soc. Jpn.* **88**, 022001 (2019).
- [14] B. Kang, S. Choi, and H. Kim, Orbital selective Kondo effect in heavy fermion superconductor  $UTe_2$ , *npj Quantum Mater.* **7**, 64 (2022).
- [15] Y. S. Eo, S. Liu, S. R. Saha, H. Kim, S. Ran, J. A. Horn, H. Hodovanets, J. Collini, T. Metz, W. T. Fuhrman, *et al.*, *c*-axis transport in  $UTe_2$ : Evidence of three-dimensional conductivity component, *Phys. Rev. B* **106**, L060505 (2022).
- [16] S. Thomas, F. Santos, M. Christensen, T. Asaba, F. Ronning, J. Thompson, E. Bauer, R. Fernandes, G. Fabbris, and P. Rosa, Evidence for a pressure-induced antiferromagnetic quantum critical point in intermediate-valence  $UTe_2$ , *Sci. Adv.* **6**, eabc8709 (2020).
- [17] D. Li, A. Nakamura, F. Honda, Y. J. Sato, Y. Homma, Y. Shimizu, J. Ishizuka, Y. Yanase, G. Knebel, J. Flouquet, *et al.*, Magnetic properties under pressure in novel spin-triplet superconductor  $UTe_2$ , *J. Phys. Soc. Jpn.* **90**, 073703 (2021).
- [18] D. Braithwaite, M. Vališka, G. Knebel, G. Lapertot, J.-P. Brison, A. Pourret, M. Zhitomirsky, J. Flouquet, F. Honda, and D. Aoki, Multiple superconducting phases in a nearly ferromagnetic system, *Commun. Phys.* **2**, 147 (2019).
- [19] S. Ran, H. Kim, I.-L. Liu, S. R. Saha, I. Hayes, T. Metz, Y. S. Eo, J. Paglione, and N. P. Butch, Enhancement and reentrance of spin triplet superconductivity in  $UTe_2$  under pressure, *Phys. Rev. B* **101**, 140503 (2020).
- [20] B. Kang, Y. Lee, L. Ke, H. Kim, and M.-H. Kim, Dual nature of magnetism driven by momentum dependent *f-d* Kondo hybridization, *Commun. Phys.* **7**, 186 (2024).
- [21] T. Hazra and P. Coleman, Triplet pairing mechanisms from Hund's-Kondo models: Applications to  $UTe_2$  and  $CeRh_2As_2$ , *Phys. Rev. Lett.* **130**, 136002 (2023).
- [22] B. Kang, C. Melnick, P. Semon, S. Rye, M. J. Han, G. Kotliar, and S. Choi, Infinite-layer nickelates as Ni-eg Hund's metals, *npj Quantum Mater.* **8**, 35 (2023).
- [23] A. Bollinger and I. Božović, Two-dimensional superconductivity in the cuprates revealed by atomic-layer-by-layer molecular beam epitaxy, *Supercond. Sci. Technol.* **29**, 103001 (2016).
- [24] Q. Si, R. Yu, and E. Abrahams, High-temperature superconductivity in iron pnictides and chalcogenides, *Nat. Rev. Mater.* **1**, 16017 (2016).
- [25] S. Choi, P. Semon, B. Kang, A. Kutepov, and G. Kotliar, ComDMFT: A massively parallel computer package for the electronic structure of correlated-electron systems, *Comput. Phys. Commun.* **244**, 277 (2019).
- [26] H. Siddiquee, C. Broyles, E. Kotta, S. Liu, S. Peng, T. Kong, B. Kang, Q. Zhu, Y. Lee, L. Ke, *et al.*, Breakdown of the scaling relation of anomalous Hall effect in Kondo lattice ferromagnet  $USbTe$ , *Nat. Commun.* **14**, 527 (2023).
- [27] B. Kang, H. Kim, Q. Zhu, and C. H. Park, Impact of *f-d* Kondo cloud on superconductivity of nickelates, *Cell Rep. Phys. Sci.* **4**, 101325 (2023).
- [28] S. Ikeda, H. Sakai, D. Aoki, Y. Homma, E. Yamamoto, A. Nakamura, Y. Shiokawa, Y. Haga, and Y. Ōnuki, Single crystal growth and magnetic properties of  $UTe_2$ , *J. Phys. Soc. Jpn.* **75**, 116 (2006).
- [29] B. Kang, Z. Brown, M.-H. Kim, H. Kim, and C. H. Park, Topological singularity-induced self-energy in strongly correlated fermion systems, arXiv preprint arXiv:2403.11382 (2024).
- [30] Q. Niu, G. Knebel, D. Braithwaite, D. Aoki, G. Lapertot, M. Vališka, G. Seyfarth, W. Knafo, T. Helm, J.-P. Brison, *et al.*, Evidence of Fermi surface reconstruction at the metamagnetic transition of the strongly correlated superconductor  $UTe_2$ , *Phys. Rev. Res.* **2**, 033179 (2020).
- [31] Y. Xu, Y. Sheng, and Y.-f. Yang, Quasi-two-dimensional fermi surfaces and unitary spin-triplet pairing in the heavy fermion superconductor  $UTe_2$ , *Phys. Rev. Lett.* **123**, 217002 (2019).
- [32] L. Miao, S. Liu, Y. Xu, E. C. Kotta, C.-J. Kang, S. Ran, J. Paglione, G. Kotliar, N. P. Butch, J. D. Denlinger, and L. A. Wray, Low energy band structure and symmetries of  $UTe_2$  from angle-resolved photoemission spectroscopy, *Phys. Rev. Lett.* **124**, 076401 (2020).
- [33] J. M. Tomczak, QSGW+DMFT: an electronic structure scheme for the iron pnictides and beyond, *J. Phys. Conf. Ser.* **592**, 012055 (2015).
- [34] K. Stöwe, Contributions to the crystal chemistry of uranium tellurides: III. temperature-dependent structural investigations on uranium ditelluride, *J. Solid State Chem.* **127**, 202 (1996).
- [35] P. Sun and G. Kotliar, Extended dynamical mean-field theory and GW method, *Phys. Rev. B* **66**, 085120 (2002).
- [36] S. Biermann, F. Aryasetiawan, and A. Georges, First-principles approach to the electronic structure of strongly correlated systems: Combining the *GW* approximation and dynamical mean-field theory, *Phys. Rev. Lett.* **90**, 086402 (2003).
- [37] F. Nilsson, L. Boehnke, P. Werner, and F. Aryasetiawan, Multi-tier self-consistent *GW*+EDMFT, *Phys. Rev. Mater.* **1**, 043803 (2017).
- [38] B. Kang, P. Semon, C. Melnick, G. Kotliar, and S. Choi, ComDMFT v.2.0: Fully self-consistent ab initio *GW*+EDMFT for the electronic structure of correlated quantum materials, arXiv preprint arXiv:2310.04613 (2023).
- [39] B. Kang, M. Kim, C. H. Park, and A. Janotti, Mott-Insulator State of  $FeSe$  as a Van der Waals 2D Material Is Unveiled, *Phys. Rev. Lett.* **132**, 266506 (2024).
- [40] A. Kutepov, K. Haule, S. Y. Savrasov, and G. Kotliar, Electronic structure of Pu and Am metals by self-consistent relativistic *GW* method, *Phys. Rev. B* **85**, 155129 (2012).
- [41] A. Kutepov, V. Oudovenko, and G. Kotliar, Linearized self-consistent quasiparticle *GW* method: application to semiconductors and simple metals, *Comput. Phys. Commun.* **219**, 407 (2017).
- [42] A. Georges, G. Kotliar, W. Krauth, and M. J. Rozenberg, Dynamical mean-field theory of strongly correlated fermion systems and the limit of infinite dimensions, *Rev. Mod. Phys.* **68**, 13 (1996).
- [43] W. Metzner and D. Vollhardt, Correlated lattice fermions in  $d = \infty$  dimensions, *Phys. Rev. Lett.* **62**, 324 (1989).
- [44] A. Georges and G. Kotliar, Hubbard model in infinite dimensions, *Phys. Rev. B* **45**, 6479 (1992).